Visualization Study on High Heat Flux Boiling and Critical Heat Flux

Satbyoul Jung [a] and Hyungdae Kim [a*]
[a]*Nuclear Engineering, Kyung Hee University, Republic of Korea*
[*]*Corresponding author: hdkims@khu.ac.kr*

1. Introduction

There have been many studies to examine the physical mechanisms of nucleation boiling and critical heat flux over several decades. Several visible and infrared-based optical techniques for time-resolved high resolution measurements for liquid-vapor phase and heater surface temperature during boiling have been introduced to understand the characteristics and mechanisms of them.

Theofanous et al. [1] used an infrared camera to measure the surface temperature and employed to study the dryout dynamics in reversible spots and the heater burnout in irreversible spots. Chu et al. [2] visualized the liquid-vapor phase distributions on a boiling surface at high heat flux boiling and critical heat flux using total reflection technique. They examined the triggering mechanisms of critical heat flux based on the observations of residual dry patch.

However, these experimental methods had limitations in simultaneously measuring instantaneous and local liquid-vapor phase and heat transfer distributions on a heated wall, which are necessary for the accurate understanding and modeling of boiling. In this study, an integrated visible and infrared-based experimental method is introduced to simultaneously measure the details of high-resolution liquid-vapor phase and heat transfer distributions on a heated wall. The dynamics and heat transfer at high heat flux boiling and critical heat flux were observed. The experiment was conducted in pool of saturated water under atmospheric pressure.

2. Experimental Technique

In this section, an integrated visible and infrared-based experimental method is introduced to simultaneously measure the temperature and phase distributions on heated wall [3].

2.1 Test sample

In order to ensure the optical techniques, we consider a thin film electric heater on a base plate as the test sample. For visible light, both the film heater and the base plate are transparent to implement total reflection technique. For infrared light, the base plate is transparent whereas the film heater is non-transparent, so that the thermal image of the heater surface can be captured from below the base plate. A good example is the combination of an Indium-Tin-Oxide (ITO) thin film heater (transparent to visible and opaque to infrared lights) and a sapphire plate (transparent to both visible and infrared lights), which is used for this study.

2.2 Experimental setup

Figure 1 shows the schematic of the optical setup. The temperature distribution of the boiling surface is measured using an infrared (IR) camera placed below the base plate. Simultaneously the phase distribution on the boiling surface is detected using the total reflection technique with a high speed video (HSV) camera. The image obtained by the total reflection technique appears dark for liquid phase and bright for vapor phase. It is noted that the prisms for total reflection should not hinder the optical path of the infrared light. The IR and HSV cameras were temporally synchronized using a function generator. The obtained each images could be spatially mapped by capturing a reference dots on test sample. In addition, another HSV camera and high flux LED were installed to visualize the bubble dynamics from side. The frame rates of IR and HSV cameras were at 500 Hz and 5 kHz, respectively.

2.3 Numerical processing for heat flux

Transient heat conduction equation for the heater plate was numerically solved by using the measured time-varying temperature distribution data of the boiling surface as boundary conditions using a commercial CFD program (ANSIS CFX) and a user defined code which was added to update the temperature boundary condition on the boiling surface for each time step.

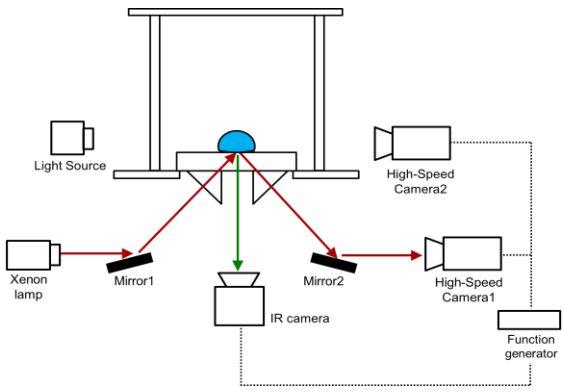

Fig. 1. Schematic of the optical system

3. Results and Discussions

Temporally and spatially synchronized visualization results for bubble dynamics, liquid-vapor phase, temperature, and heat flux distributions is presented as increasing the applied heat flux. All the data presented in this paper were obtained for bubble nucleate boiling of saturated water under atmospheric pressure. Figure 2 shows the boiling curve for which the synchronized TR and IR visualization test was performed. The details of observations at high heat flux including the critical heat flux will be discussed.

Figure 3 shows the experimental results for growth and merging of bubbles during nucleate boiling at the medium heat flux, 786 kW/m^2 (q''/q''_{CHF}=0.93). They are arranged in order of bubble shape, phase distribution, and temperature and heat flux distributions with triple contact line which is obtained from the phase distribution.

Several bubble nucleates at 0.222 s and grow fast, creating a wide extended microlayer. The area shows very high heat flux over 1.5 MW/m^2, obviously due to evaporation of microlayer [3]. In contrast, very low heat fluxes close to zero are observed at the dry areas where the microlayer was completely evaporated out. It is consistent with the observation of Jung et al. [4]. Even after the exhaustion of the microlayer, thin lines with relatively high heat fluxes to the surrounding areas continuously remained along the periphery of the dry patch. The line corresponds to the triple contact line (TCL). As expected, the relatively high heat flux is resulted from evaporation of liquid at the triple contact line. However, the TCL evaporation heat transfer does not seem to solely play a role in the high heat flux nucleate boiling mechanism.

After 0.222 s, the close dry patches are merged together and the resulting large dry patch is formed. The local temperature inside the dry patch increased from 115 to 123°C during the life time of the patch. The locally heated area, so-called hot patch, was cooled down when liquid forced into the dry area. At the moment of the rewetting (or quenching) of the large dry/hot patch area, several bubbles nucleate on the wetting region, which is consistent with the observation of Chu et al. [2].

Approaching to CHF, large dry patches repeatedly expand and contract, which is exactly same as the behavior at lower heat fluxes and constantly repeated as seen in Fig. 4. At a certain moment of rewetting, a few subsequent bubbles immediately nucleate and a dry patch is generated at the same point before the thermal energy accumulated on the hot spot is sufficiently relieved. Because the newly generated thermal energy in the dry area is added up to the remained one, the next rewetting again fails to completely extinguish the hot patch. In this way, the large dry/hot patch with the residual dry patch leads the way toward CHF condition. Finally, the patch irreversibly grows and covers the entire heater surface in an instant, resulting in a transition to film boiling.

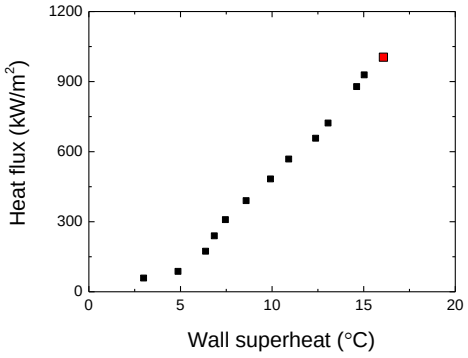

Fig. 2. Boiling curve of saturated water under atmospheric pressure

4. Conclusions

Liquid-vapor phase, temperature, and heat flux distributions on the heated surface were measured during pool boiling of water using the integrated total reflection and infrared thermometry technique. Qualitative examination of the data for high heat flux boiling and CHF was performed. The main contributions of this work are summarized below.

- The existence and behavior of dry patches lead the way toward CHF condition. Therefore, the mechanistic modeling of the CHF phenomenon necessarily needs to include the physical parameters related to dynamics of the large dry patch such as life time and size.
- In addition to the dynamic behavior of the dry patch, the thermal behavior of the hot patch is also important. Even though the dry area was rewetted, the stored thermal energy in the hot patch can be remained if the rewetting time is short and the subsequent dry patch is regenerated quickly.

REFERENCES

[1] T. G. Theofanous, J. P. Tu, A. T. Dinh, T. N. Dinh, The Boiling Crisis Phenomenon, Experimental Thermal Fluid Science, P.I: 775-792, P.II: 793-810, Vol. 26, 2002.
[2] I. Chu, H. C. No, C. Song, Visualization of boiling structure and critical heat flux phenomenon for a narrow heating surface in a horizontal pool of saturated water, Int. J. Heat and Mass Transfer, Vol. 62, pp. 142–152, 2013.
[3] S. Jung, H. Kim, An experimental method to simultaneously measure the dynamics and heat transfer associated with a single bubble during nucleate boiling on a horizontal surface, Int. J. Heat and Mass Transfer, Vo. 73, pp. 365-375, 2014.
[4] J. Jung, S. J. Kim, J. Kim, Observations of the critical heat flux process during pool boiling of FC-72, J. Heat Transfer, Vol. 136, 04150, 2014.

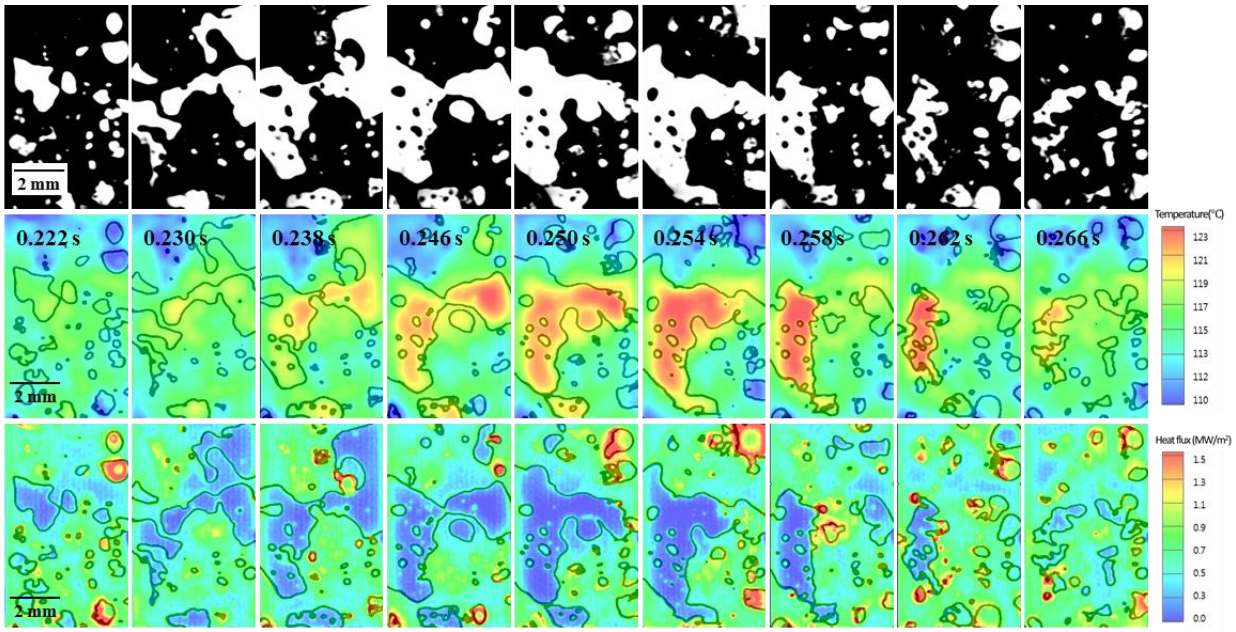

Fig. 3. Visualization result of bubble shape, liquid-vapor phase, temperature and heat flux distributions on the boiling surface at 786 kW/m^2 (q''/q''_{CHF} =0.93)

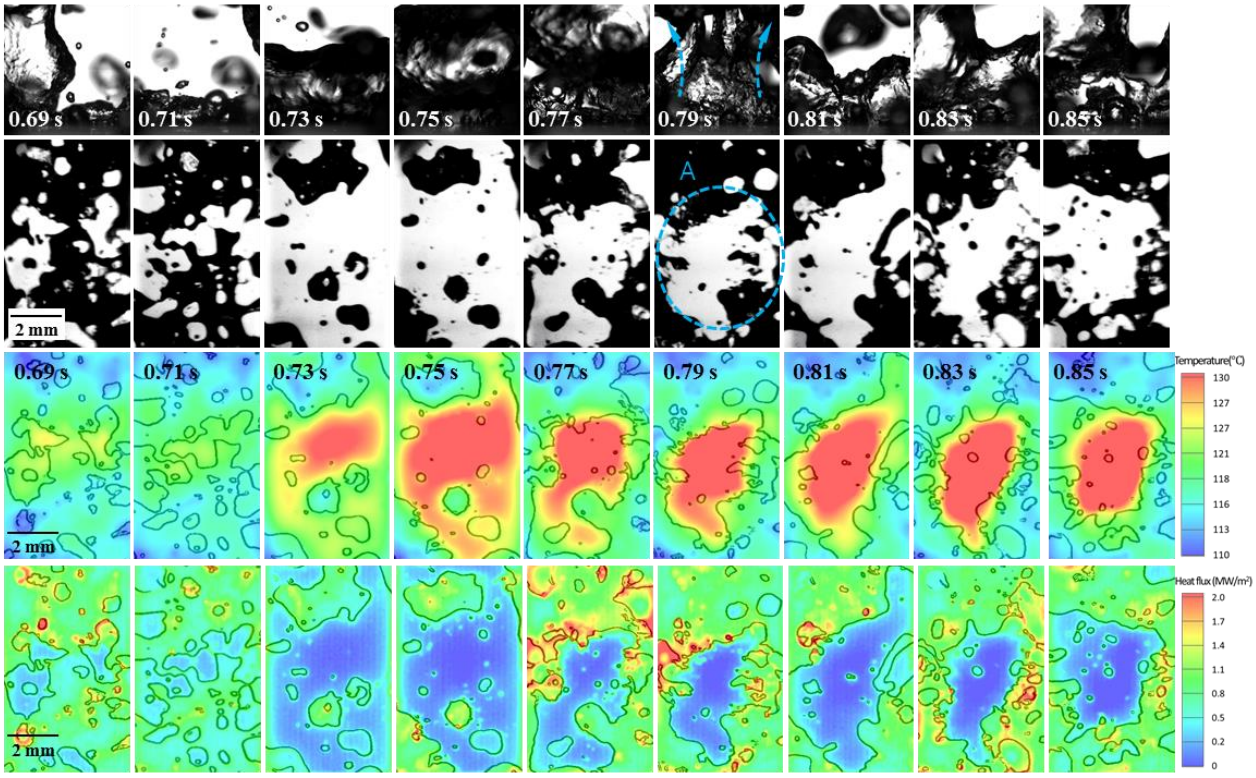

Fig. 4. Visualization result of bubble shape, liquid-vapor phase, temperature and heat flux distributions on the boiling surface at critical heat flux, q''=845 kW/m^2